

Article

Superconvergence of Modified Nonconforming Cut Finite Element Method for Elliptic Problems

Xiaoxiao He ¹ and Fei Song ^{2,*}

¹ School of Science, Nanjing University of Posts and Telecommunications, Nanjing 210023, China; hxx@njupt.edu.cn

² College of Science, Nanjing Forestry University, Nanjing 210037, China

* Correspondence: songfei@njfu.edu.cn

Abstract: In this work, we aim to explore the superconvergence of a modified nonconforming cut finite element method with rectangular meshes for elliptic problems. Boundary conditions are imposed via the Nitsche's method. The superclose property is proven for rectangular meshes. Moreover, a postprocessing interpolation operator is introduced, and it is proven that the postprocessed discrete solution converges to the exact solution, with a superconvergence rate $O(h^{3/2})$. Finally, numerical examples are provided to support the theoretical analysis.

Keywords: superconvergence; modified nonconforming cut finite element; rectangular meshes

MSC: 65N12; 65N15; 65N30

1. Introduction

Boundaries/interfaces with time or involving complex geometries arise in many engineering applications and physical phenomena problems. Cut finite element methods (CutFEM) have been developed to solve PDEs whose solutions involve jumps, kinks, singularities and other locally non-smooth features within elements. This method not only retains the accuracy and robustness of a standard finite element method, but also relaxes the mesh, which is independent of the geometric description. Over the past few decades, cut finite element methods have been applied to many problems [1–6]. We also refer to the overview article [7] and the references therein.

Note that superconvergence of the finite element method is quite popular in practice, and several types have been studied in the past few decades. There are two main techniques within the framework of superconvergence. One technique is the interpolation approximation, which has two ingredients: the supercloseness between the numerical solution and the finite element canonical interpolant, and the global superconvergence between the exact solution and a postprocessed solution. This technique has been studied for conforming finite elements [8–11] and nonconforming finite elements [12,13]. The other one uses some equivalences, and involves translating the superconvergence of the original problems into the superconvergence of some mixed problems—for example, the equivalence between the Crouzeix–Raviart method and the lower order Raviart–Thomas (RT) method for the Poisson equation [14], and the equivalence between the nonconforming Rannacher–Turek (NCRT) element and RT element for elliptic equations [15].

For the NCRT element, based on the interpolation approximation technique, it has been shown in [12] that the supercloseness between the numerical solution and the finite element interpolation holds only under square meshes. To overcome this barrier, many modified NCRT elements [12,13,16] have been proposed. In this work, we study the cut finite element method, based on the five-node nonconforming element developed in [12,13]. The main contribution is that a postprocessing operator is designed, and the superconvergence



Citation: He, X.; Song, F.

Superconvergence of Modified Nonconforming Cut Finite Element Method for Elliptic Problems.

Mathematics **2024**, *12*, 2595. <https://doi.org/10.3390/math12162595>

Academic Editor: Patricia J. Y. Wong

Received: 19 July 2024

Revised: 20 August 2024

Accepted: 20 August 2024

Published: 22 August 2024



Copyright: © 2024 by the authors. Licensee MDPI, Basel, Switzerland. This article is an open access article distributed under the terms and conditions of the Creative Commons Attribution (CC BY) license (<https://creativecommons.org/licenses/by/4.0/>).

order $O(h^{3/2})$ is proven for elliptic problems based on the nonconforming CutFEM under rectangular meshes.

The remainder of this paper is organized as follows. In Section 2, we formulate the modified nonconforming CutFEM. The supercloseness is presented in Section 3. A postprocessing operator and the global superconvergence are analyzed in Section 4. Some numerical results are shown in Section 5 to verify the theoretical results. The conclusions are given in the last section. Throughout this paper, C is used to denote generic positive constants, which are independent of h , the location of the boundary to the mesh. Moreover, $A \lesssim B$ stands for $A \leq CB$.

2. The Model Problem and the Finite Element Formulation

Consider the following elliptic problem with a bounded and simply connected domain $\Omega \subset \mathbb{R}^2$ under a smooth boundary $\Gamma = \partial\Omega$:

$$\begin{cases} -\Delta u = f & \text{in } \Omega, \\ u = g & \text{on } \partial\Omega, \end{cases} \tag{1}$$

where f is a smooth function, and $g \in H^{\frac{1}{2}}(\Gamma)$ is the Dirichlet boundary function prescribed on Γ .

Remark 1. For $f \in L^2(\Omega)$ and $g \in H^{\frac{1}{2}}(\Gamma)$, it is well known that the variational formulation of (1) has a unique solution $u \in H^1(\Omega)$. In the following analysis of superconvergence, we assume that $g \in H^{\frac{5}{2}}(\Gamma)$ for the solution $u \in H^3(\Omega) \cap W^{2,\infty}(\Omega)$.

For domain Ω , we first define a fictitious domain $\tilde{\Omega}$, such that $\Omega \subset \tilde{\Omega}$. Let $\{\mathcal{T}_h\}$ be a family of non-overlapping rectangles that cover the domain $\tilde{\Omega}$. For any $K \in \mathcal{T}_h$, we define h_K as $\text{diam}(K)$, and denote $h := \max_{K \in \mathcal{T}_h} h_K$. Note that any element $K \in \mathcal{T}_h$ is considered closed. Define the set of cut elements by $G_h^\Gamma := \{K \in \mathcal{T}_h : K \cap \Gamma \neq \emptyset\}$. In particular, for $K \in G_h^\Gamma$, we denote $\Gamma_K = K \cap \Gamma$, $\mathcal{T}_h^\Omega := \{K \in \mathcal{T}_h : K \cap \Omega \neq \emptyset\}$ and $\Omega_h := \cup_{K \in \mathcal{T}_h^\Omega} K$. Denote the set of all interior edges of \mathcal{T}_h^Ω by ε_h . Denote uncut and cut edges by ε_h^{nc} and ε_h^{cut} , respectively, which are defined as $\varepsilon_h^{nc} := \{e \in \varepsilon_h : e = \partial K_l \cap \partial K_r, K_l, K_r \in \mathcal{T}_h, \text{ and } e \subset \Omega\}$, and $\varepsilon_h^{cut} := \{\tilde{e} = e \cap \Omega : e = \partial K_l \cap \partial K_r, K_l, K_r \in G_h^\Gamma\}$. Further, the set of extended edges is denoted by

$$\varepsilon_h^\Gamma := \{e = \partial K_l \cap \partial K_r : K_l, K_r \in \mathcal{T}_h, K_l \text{ or } K_r \in G_h^\Gamma\}.$$

Define $\|\cdot\|_{h,\Omega_h}^2 := \sum_{K \in \mathcal{T}_h^\Omega} \|\nabla \cdot\|_{L^2(K)}^2$.

We define a weak space:

$$V := \{v \in L^2(\Omega_h) : v \in H^2(K), \forall K \in \mathcal{T}_h^\Omega\}.$$

Let $\hat{K} = [-1, 1] \times [-1, 1]$ denote the reference element with four vertices $\hat{a}_1 = (-1, -1)$, $\hat{a}_2 = (1, -1)$, $\hat{a}_3 = (1, 1)$ and $\hat{a}_4 = (-1, 1)$. Denote the bilinear function F_K as an isomorphism from \hat{K} to K by

$$x = \sum_i^4 x_i N_i(\xi, \eta), \quad y = \sum_i^4 y_i N_i(\xi, \eta), \quad (\xi, \eta) \in \hat{K},$$

where $(x_i, y_i), i = 1, 2, 3, 4$ are four vertices of element K , and $N_i(\xi, \eta), i = 1, 2, 3, 4$ are the basis functions of the standard conforming bilinear finite element space, which can be written as

$$\begin{aligned} N_1(\xi, \eta) &= \frac{1}{4}(1 - \xi)(1 - \eta), & N_2(\xi, \eta) &= \frac{1}{4}(1 + \xi)(1 - \eta), \\ N_3(\xi, \eta) &= \frac{1}{4}(1 + \xi)(1 + \eta), & N_4(\xi, \eta) &= \frac{1}{4}(1 - \xi)(1 + \eta). \end{aligned}$$

Denote the finite element space of modified nonconforming elements with support in Ω_h by

$$V_h := \left\{ v \in L^2(\Omega_h) : v|_K \in \tilde{Q}_{NCRT}(K), \int_e [v] ds = 0, \forall e \in \varepsilon_h \right\},$$

where $\tilde{Q}_{NCRT}(K) := \{q = \hat{q} \circ F_K^{-1} | \hat{q} \in span < 1, \zeta, \eta, \zeta^2, \eta^2 >, [v]|_e = v|_{K_l} - v|_{K_r} \text{ if } e = \partial K_l \cap \partial K_r\}$.

We now give the finite element formulation based on the weak formulation of Problem (1). Firstly, the average $\{v\}$ on the cut edges \tilde{e} is defined by

$$\{v\} = \frac{1}{2} v_l|_{\tilde{e}} + \frac{1}{2} v_r|_{\tilde{e}},$$

with $v_j = v|_{K_j}, j = l, r, K_l, K_r \in G_h^\Gamma$.

The modified nonconforming cut finite element method is to find $u_h \in V_h$ such that

$$A_h(u_h, v_h) = L_h(v_h), \quad \forall v_h \in V_h, \tag{2}$$

where $A_h(\cdot, \cdot)$ is the bilinear form on $(V + V_h) \times (V + V_h)$ and $L_h(\cdot)$ is the linear function on $V + V_h$, defined by

$$\begin{aligned} A_h(u, v) = & \sum_{K \in \mathcal{T}_h^\Omega} \int_{K \cap \Omega} \nabla u \cdot \nabla v - \sum_{K \in G_h^\Gamma} \int_{\Gamma_K} (\nabla u \cdot \mathbf{n} v + \nabla v \cdot \mathbf{n} u) \\ & + \sum_{K \in G_h^\Gamma} \frac{\gamma_0}{h} \int_{\Gamma_K} uv - \sum_{\tilde{e} \in \varepsilon_h^{cut}} \int_{\tilde{e}} (\{\nabla u \cdot \mathbf{n}_{\tilde{e}}\}[v] + \{\nabla v \cdot \mathbf{n}_{\tilde{e}}\}[u]) \\ & + \sum_{\tilde{e} \in \varepsilon_h^{cut}} \frac{\gamma_1}{h} \int_{\tilde{e}} [u][v] + \sum_{e \in \varepsilon_h^\Gamma} h \int_e [\nabla u][\nabla v], \end{aligned} \tag{3}$$

and

$$L_h(v) = \int_\Omega f v + \sum_{K \in G_h^\Gamma} \int_{\Gamma_K} g \left(\nabla v \cdot \mathbf{n} + \frac{\gamma_0}{h} v \right), \tag{4}$$

where \mathbf{n} is the unit outward normal vector on the boundary Γ , and $\gamma_i (i = 0, 1)$ are positive numbers.

We introduce the energy norm on the space $V + V_h$ as

$$\|v\|_h^2 := \sum_{K \in \mathcal{T}_h^\Omega} \|\nabla v\|_{L^2(K \cap \Omega)}^2 + \|v\|_{h,\Gamma}^2 + \|v\|_{cut}^2 + \sum_{e \in \varepsilon_h^\Gamma} h \|\nabla v\|_{L^2(e)}^2, \tag{5}$$

with

$$\|v\|_{h,\Gamma}^2 := \frac{1}{h} \sum_{K \in G_h^\Gamma} \|v\|_{L^2(\Gamma_K)}^2 \text{ and } \|v\|_{cut}^2 := \sum_{\tilde{e} \in \varepsilon_h^{cut}} \frac{1}{h} \|[v]\|_{L^2(\tilde{e})}^2.$$

From the proof of Lemma 6 in [2], the following inequality can be directly obtained.

Lemma 1. *Suppose that h is sufficiently small. For any $v_h \in V_h$, we have*

$$\|v_h\|_{h,\Omega_h}^2 \lesssim \|v_h\|_{h,\Omega}^2 + \sum_{e \in \varepsilon_h^\Gamma} h \|\nabla v\|_{L^2(e)}^2,$$

where $\|v_h\|_{h,\Omega}^2 = \sum_{K \in \mathcal{T}_h^\Omega} \|\nabla v\|_{L^2(K \cap \Omega)}^2$.

To analyze the convergence and superconvergence, we need an extension result (see Chapter VI, Section 2 of [17], or Chapter 6 of [18]). We continuously extend the solution $u \in H^3(\Omega) \cap W^{2,\infty}(\Omega)$ of (1) to \mathbb{R}^2 to obtain a function $\tilde{u} \in H^3(\mathbb{R}^2) \cap W^{2,\infty}(\mathbb{R}^2)$, such that

$$\tilde{u}|_{\Omega} = u, \quad \|\tilde{u}\|_{H^j(\mathbb{R}^2)} \lesssim \|u\|_{H^j(\Omega)}, \quad j = 0, 1, 2, 3, \tag{6}$$

and

$$\|\tilde{u}\|_{W^{2,\infty}(\mathbb{R}^2)} \lesssim \|u\|_{W^{2,\infty}(\Omega)}. \tag{7}$$

It is easy to obtain the following inconsistency equation:

$$A_h(u - u_h, v_h) = \sum_{e \in \mathcal{E}_h^{nc}} \int_e \nabla u \cdot \mathbf{n}_e [v_h]. \tag{8}$$

Assume that γ_0 and γ_1 are large enough; it is easy to find that the coercivity of $A_h(\cdot, \cdot)$ holds, which can be proven similarly to Theorems 4.1 and 4.2 of [19]. Then, the a priori error estimate for the modified nonconforming CutFEM holds:

$$\|u - u_h\|_{L^2(\Omega)} + h \|u - u_h\|_h \lesssim h^2 \|u\|_{H^2(\Omega)}. \tag{9}$$

Estimate (9) implies that (2) is a first order in energy norm $\|\cdot\|_h$. Therefore, an improved $1 + s, s > 0$ order for the recovery-type error estimate indicates superconvergence. Moreover, if the $\|\cdot\|_h$ -distance between two functions is $O(h^{1+s})$, we say that they are superclose.

3. Supercloseness Analysis

In this section, we will show the supercloseness result between the gradient of the finite element solution and the gradient of the interpolation of the exact solution. Firstly, for any element K , define a local interpolation operator by $\int_e \Pi_K v = \int_e v$ and $\int_K \Pi_K v = \int_K v$, where $e \subset \partial K$. Denote by Π_h the interpolation operator over V_h by $\Pi_h v := (\Pi_h \tilde{v})|_{\Omega}$ and $\Pi_h v|_K = \Pi_K v$. From the interpolation theory in [20] and the above extension properties, the following approximation estimate holds:

$$\sum_{K \in \mathcal{T}_h} |u - \Pi_h u|_{W^{l,p}(K)}^2 \lesssim h^{2-l} |\tilde{u}|_{W^{2,p}(\mathbb{R}^2)} \lesssim h^{2-l} |u|_{W^{2,p}(\Omega)}, \tag{10}$$

where $l = 0, 1$ and $1 \leq p \leq \infty$.

For element $K \in \mathcal{T}_h \setminus \mathcal{G}_h^F$ and $v_h \in V_h$, $\nabla \cdot (\nabla v_h)$ and $(\nabla v_h \cdot \mathbf{n}_K)|_{\partial K}$ are constants, and then $\int_K (u - \Pi_h u) \nabla \cdot (\nabla v_h) = 0$ and $\int_{\partial K} (u - \Pi_h u) \nabla v_h \cdot \mathbf{n}_K = 0$, through the definition of Π_h . Similarly to the proof of Theorem 3.1 of [21], we have the following Lemma.

Lemma 2. *Let u be the solution of the interface problem, and $\Pi_h u$ be the interpolation of u , defined as above. If $u \in W^{2,\infty}(\Omega)$, then for all $v_h \in V_h$,*

$$A_h(u - \Pi_h u, v_h) \lesssim h^{3/2} \|u\|_{2,\infty,\Omega} \|v_h\|_h.$$

Theorem 1. *Let u_h be the finite element solution of the discrete problem, and $\Pi_h u$ be the interpolation of u . If $u \in H^3(\Omega) \cap W^{2,\infty}(\Omega)$, then*

$$\|u_h - \Pi_h u\|_h \leq C \left(h^2 \|u\|_{3,\Omega} + h^{3/2} \|u\|_{2,\infty,\Omega} \right).$$

Proof. Using the coercivity of $A_h(\cdot, \cdot)$, we have

$$\begin{aligned} \|u_h - \Pi_h u\|_h^2 &\lesssim A_h(u_h - \Pi_h u, u_h - \Pi_h u) \\ &= A_h(u - \Pi_h u, u_h - \Pi_h u) - A_h(u - u_h, u_h - \Pi_h u). \end{aligned} \tag{11}$$

From Lemma 2, the first term on the right hand can be estimated via

$$A_h(u - \Pi_h u, u_h - \Pi_h u) \leq Ch^{3/2} \|u\|_{2,\infty,\Omega} \| \|u_h - \Pi_h u\|_h. \tag{12}$$

From Lemma 3.1 of [12], the following consistency error estimate holds:

$$A_h(u - u_h, u_h - \Pi_h u) \leq Ch^2 \|u\|_{3,\Omega} \| \|u_h - \Pi_h u\|_h. \tag{13}$$

Combining (12) with (13), we complete the proof. \square

Remark 2. From the definition of $\| \cdot \|_h$, Lemma 1, and Theorem 1, we obtain

$$\|u_h - \Pi_h u\|_{h,\Omega_h} \lesssim h^2 \|u\|_{3,\Omega} + h^{3/2} \|u\|_{2,\infty,\Omega}. \tag{14}$$

4. Postprocessing and Superconvergence

In this section, we will use a postprocessing operator defined in [13], and apply it to our fictitious domain. The global superconvergence for the modified nonconforming cut finite element method to elliptic problems will be analyzed. For this purpose, we assume that \mathcal{T}_h is obtained from \mathcal{T}_{2h} by dividing each element M of \mathcal{T}_{2h} into four congruent rectangles $K_i, i = 1, 2, 3, 4$. Define an operator I_{2h} on \mathcal{T}_{2h} , $I_{2h}|_M = I_M$, and define the local operator $I_M : L^1(M) \rightarrow P_2(M)$ by

$$\int_{e_i} (I_M u - u) = 0, i = 1, 2, 3, 4; \int_{K_1 \cup K_3} (I_M u - u) = 0; \int_{K_2 \cup K_4} (I_M u - u) = 0,$$

where $e_i, i = 1, 2, 3, 4$ are four edges of M . From Lemma 3.2 of [13], we obtain the following Lemma, which presents the properties of operator I_{2h} .

Lemma 3. The interpolation operator I_{2h} satisfies

$$I_{2h} \Pi_h u = I_{2h} u, \| (u - I_{2h} u) \|_{2h,\tilde{\Omega}} \lesssim h^2 \|u\|_{3,\tilde{\Omega}}, \| I_{2h} v_h \|_{2h,\tilde{\Omega}} \lesssim \|v_h\|_{2h,\tilde{\Omega}}.$$

Now, we give some notations. For partition \mathcal{T}_{2h} , we define $\mathcal{T}_{2h}^\Omega := \{M \in \mathcal{T}_{2h} : M \cap \Omega \neq \emptyset\}$ and $\Omega_{2h} := \cup_{M \in \mathcal{T}_{2h}^\Omega} M$. Let $G_{2h}^\Gamma := \{M \in \mathcal{T}_{2h} : M \not\subseteq \Omega_h\}$. Note that there might exist an element $K \in \mathcal{T}_h$ which is not in \mathcal{T}_h^Ω for $K \subset M$ and $M \in G_{2h}^\Gamma$ (see Figure 1 for an illustration). For each element $M \in G_{2h}^\Gamma$, in order to obtain superconvergence, we need expand the value from Ω into M . For $K \subset M$ but $K \cap \Omega = \emptyset$, there is $K' \subset M$ and $K' \subset \Omega_h$. Let $P_K : L^2(K) \rightarrow \tilde{Q}_{NCRT}(K)$ be the $L^2(K)$ projection. Take

$$P_{K',K} v := P_K(\widetilde{v_h|_{K'}}) \in \tilde{Q}_{NCRT}(K)$$

with

$$P_{K',K} v = \sum_{i=1}^5 \widehat{v}_{K,i}^{K'} \phi_{K,i}$$

where \widehat{v}_h is the continuous extension of v_h and $\phi_{K,i}$ is the basis function of $\tilde{Q}_{NCRT}(K)$. Further, we define

$$Q_K v = \sum_{i=1}^5 \langle \widehat{v}_{K,i} \rangle \phi_{K,i}$$

where the average is the convex combination

$$\langle \widehat{v}_{K,i} \rangle = \sum_{m \in I_K} \omega_{K^m} \widehat{v}_{K,i}^{K^m}$$

with weights ω_{K^m} , such that $0 \leq \omega_{K^m} \leq 1$ and $\sum_m \omega_{K^m} = 1$, and $I_K = \{m : K_m \subset \Omega_h \text{ for } K \in M, K \cap \Omega = \emptyset, K_m \in M\}$. For $v \in V_h$, let $Q_h v|_K = Q_K v$. It is easy to find that

$$Q_h \Pi_h v = \Pi_h v \quad \text{and} \quad \|Q_h v_h\|_{2h, \Omega_{2h}} \lesssim \|v_h\|_{h, \Omega_h}.$$

For $v \in V_h$, we define a postprocessing operator \mathcal{J}_{2h} by $\mathcal{J}_{2h} v := I_{2h} Q_h v$. Then, we can obtain the following main superconvergence result in this work.

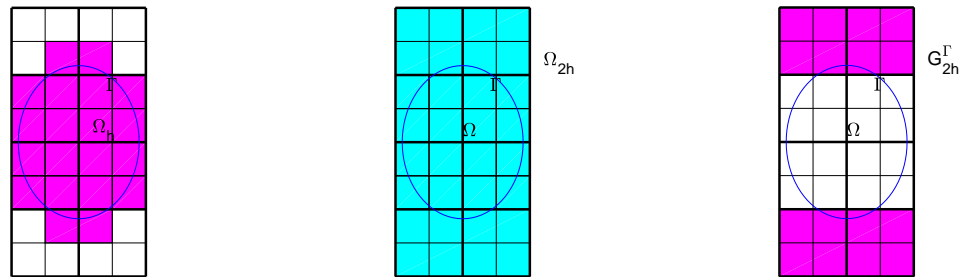


Figure 1. Illustration of definitions of \mathcal{T}_h^Ω , \mathcal{T}_{2h}^Ω , Ω_h , Ω_{2h} and G_{2h}^Γ for domain Ω . Partitions \mathcal{T}_h^Ω (fine meshes) and \mathcal{T}_{2h}^Ω (coarse meshes) of domain Ω . Left: elements in Ω_h (magenta area). Middle: elements in Ω_{2h} (cobalt blue area). Right: elements in G_{2h}^Γ (magenta area).

Theorem 2. Let u and u_h be the solutions of (1) and (2), respectively. Assume that $u \in W^{2,\infty}(\Omega) \cap H^3(\Omega)$, then

$$\|u - \mathcal{J}_{2h} u_h\|_{2h, \Omega} \lesssim h^2 \|u\|_{3, \Omega} + h^{3/2} \|u\|_{2, \infty, \Omega}.$$

Proof. We decompose $u - \mathcal{J}_{2h} u_h$ as $(u - \mathcal{J}_{2h} \Pi_h u) + (\mathcal{J}_{2h} \Pi_h u - \mathcal{J}_{2h} u_h)$. Then, the triangle inequality implies that

$$\begin{aligned} \|(u - \mathcal{J}_{2h} u_h)\|_{2h, \Omega} &\leq \|(u - \mathcal{J}_{2h} \Pi_h u)\|_{2h, \Omega} + \|(\mathcal{J}_{2h} \Pi_h u - \mathcal{J}_{2h} u_h)\|_{2h, \Omega} \\ &= \|(u - I_{2h} u)\|_{2h, \Omega} + \|(I_{2h} Q_h \Pi_h u - I_{2h} Q_h u_h)\|_{2h, \Omega}, \end{aligned} \tag{15}$$

where the last equality uses the definition of \mathcal{J}_{2h} and Lemma 3, and then we obtain $\mathcal{J}_{2h} \Pi_h u = I_{2h} Q_h \Pi_h u = I_{2h} \Pi_h u = I_{2h} u$. From Lemma 3 and the extension properties, we have

$$\|u - I_{2h} u\|_{2h, \Omega} \leq Ch^2 \|u\|_{3, \Omega}. \tag{16}$$

Using Lemma 3, we obtain

$$\begin{aligned} &\|I_{2h} Q_h \Pi_h u - I_{2h} Q_h u_h\|_{2h, \Omega} \\ &\leq C \|Q_h \Pi_h u - Q_h u_h\|_{2h, \Omega_{2h}} \leq C \|\Pi_h u - u_h\|_{h, \Omega_h}, \end{aligned} \tag{17}$$

and together with (14), the following estimate holds

$$\|I_{2h} Q_h \Pi_h u - I_{2h} Q_h u_h\|_{2h, \Omega} \lesssim h^2 \|u\|_{3, \Omega} + h^{3/2} \|u\|_{2, \infty, \Omega}. \tag{18}$$

Finally, the proof is directly obtained from (16)–(18). \square

5. Numerical Examples

In this section, we will consider several numerical examples to verify the theoretical results given in the previous section. In these examples, we will test the convergence rate, supercloseness result and superconvergence rate based on square meshes and different rectangular meshes. We summarize our experimental results in tables, displaying the following errors: $De := \|u - u_h\|_{h, \Omega}$, $D^\Pi e := \|u_h - \Pi_h u\|_{h, \Omega}$ and $D^\mathcal{J} e := \|u - \mathcal{J}_{2h} u_h\|_{2h, \Omega}$.

5.1. Example 1

In this example, we consider the elliptic problem with a circular boundary with center $(0, 0)$ and radius $r = 1/2$. Define domain $\Omega = \{(x, y) : x^2 + y^2 < r^2\}$. Choose the fictitious domain $\tilde{\Omega} = [-0.5, 0.5] \times [-0.5, 0.5]$, and let f be chosen such that the exact solution is $u(x, y) = (x^2 - x)(y^2 - y)$. The performance for errors of De , $D^{\Pi}e$ and $D^{\mathcal{J}}e$ with square and rectangular meshes are shown in Table 1. Firstly, it shows errors of De , $D^{\Pi}e$, and $D^{\mathcal{J}}e$ versus square meshes with $h_x = h_y = 1/8, 1/16, 1/32, 1/64$ and $\gamma_0 = \gamma_1 = 100$, respectively. It is observed that our formulation converges with the optimal rate $O(h)$ for De , and with rate $O(h^{3/2})$ for $D^{\Pi}e$ and $D^{\mathcal{J}}e$, which support Theorems 1 and 2. Secondly, the performance for errors of De , $D^{\Pi}e$ and $D^{\mathcal{J}}e$, based on two different rectangular meshes, are also tested. It is shown that the convergence rate of De is $O(h)$, and the convergence orders for $D^{\Pi}e$ and $D^{\mathcal{J}}e$ are $O(h^{3/2})$, which are also coincide with the theoretical analysis.

Table 1. Rates of errors for Example 1 based on square and rectangular meshes with penalty parameters $\gamma_0 = \gamma_1 = 100$.

h_x	h_y	De	Rate	$D^{\Pi}e$	Rate	$D^{\mathcal{J}}e$	Rate
1/8	1/8	9.3335×10^{-2}		8.6752×10^{-2}		8.7346×10^{-2}	
1/16	1/16	4.1432×10^{-2}	1.1716	3.4709×10^{-2}	1.3215	3.6997×10^{-2}	1.2393
1/32	1/32	1.8062×10^{-2}	1.1977	1.2783×10^{-2}	1.4410	1.4339×10^{-2}	1.3674
1/64	1/64	8.1059×10^{-3}	1.1559	4.5268×10^{-3}	1.4977	5.1910×10^{-3}	1.4658
1/4	1/8	1.4864×10^{-1}		1.4406×10^{-1}		1.5410×10^{-1}	
1/8	1/16	7.0590×10^{-2}	1.0742	6.3422×10^{-2}	1.1836	7.0242×10^{-2}	1.1335
1/16	1/32	3.0848×10^{-2}	1.1942	2.4337×10^{-2}	1.3818	2.6597×10^{-2}	1.4010
1/32	1/64	1.3424×10^{-2}	1.2003	8.5553×10^{-3}	1.5082	9.9456×10^{-3}	1.4191
1/8	1/6	1.1737×10^{-1}		1.1222×10^{-1}		1.0300×10^{-1}	
1/16	1/12	5.1093×10^{-2}	1.1998	4.4336×10^{-2}	1.3398	4.4650×10^{-2}	1.2060
1/32	1/24	2.2139×10^{-2}	1.2065	1.6559×10^{-2}	1.4208	1.7724×10^{-2}	1.3329
1/64	1/48	9.8307×10^{-3}	1.1712	5.9211×10^{-3}	1.4836	6.5601×10^{-3}	1.4339

5.2. Example 2

In this example, we consider an elliptic boundary condition. The boundary curve is the zero level set of the following function: $\varphi(x, y) = \frac{x^2}{(3/4)^2} + \frac{y^2}{(1/2)^2} - 1$. Define domain $\Omega = \{(x, y) : \varphi(x, y) < 0\}$, and let the fictitious domain $\tilde{\Omega} = [-1, 1] \times [-0.5, 0.5]$. We choose the exact solution $u(x, y) = e^{xy}$. The numerical results for De , $D^{\Pi}e$, and $D^{\mathcal{J}}e$, based on square and rectangular meshes with $\gamma_0 = \gamma_1 = 100$, are presented in Table 2, which shows the same convergence, supercloseness, and superconvergence rates as the theoretical analysis.

Table 2. Rates of errors for Example 2 based on square and rectangular meshes with penalty parameters $\gamma_0 = \gamma_1 = 100$.

h_x	h_y	De	Rate	$D^{\Pi}e$	Rate	$D^{\mathcal{J}}e$	Rate
1/8	1/8	9.0498×10^{-2}		8.0253×10^{-2}		8.7898×10^{-2}	
1/16	1/16	3.8709×10^{-2}	1.2252	2.9733×10^{-2}	1.4324	3.3166×10^{-2}	1.4061
1/32	1/32	1.7297×10^{-2}	1.1621	1.0919×10^{-2}	1.4452	1.2686×10^{-2}	1.3864
1/64	1/64	7.8501×10^{-3}	1.1397	3.7896×10^{-3}	1.5267	4.3814×10^{-3}	1.5337
1/4	1/8	1.4929×10^{-1}		1.3847×10^{-1}		1.4334×10^{-1}	
1/8	1/16	6.3781×10^{-2}	1.2269	5.2454×10^{-2}	1.4004	5.1589×10^{-2}	1.4743
1/16	1/32	2.7873×10^{-2}	1.1942	1.9036×10^{-2}	1.4622	2.0169×10^{-2}	1.3548
1/32	1/64	1.2656×10^{-2}	1.1390	6.7447×10^{-3}	1.4969	7.4012×10^{-3}	1.4463

Table 2. Cont.

h_x	h_y	De	Rate	$D^{\Pi}e$	Rate	$D^{\mathcal{J}}e$	Rate
1/8	1/4	1.5692×10^{-1}		1.4741×10^{-1}		1.7173×10^{-1}	
1/16	1/8	7.0478×10^{-2}	1.1547	6.0883×10^{-2}	1.2757	7.0293×10^{-2}	1.2887
1/32	1/16	2.9559×10^{-2}	1.2535	2.1598×10^{-2}	1.4951	2.6111×10^{-2}	1.4287
1/64	1/32	1.3058×10^{-2}	1.1786	7.5276×10^{-3}	1.5206	9.2699×10^{-3}	1.4940

5.3. Example 3

In this example, we choose a more complicated boundary. The boundary curve is the zero level set of the following function: $\varphi(x, y) = (3(x^2 + y^2)^2 - x)^2 - x^2 - y^2 + 0.02$. Let domain $\Omega = \{(x, y) : \varphi(x, y) < 0\}$, and the fictitious domain $\tilde{\Omega} = [-0.25, 0.75] \times [-0.5, 0.5]$. The exact solution is set to be $u(x, y) = \sin(\pi x)\sin(\pi y)$. Table 3 displays the convergence rates of De , $D^{\Pi}e$, and $D^{\mathcal{J}}e$ for our formulation based on square and rectangular meshes with $\gamma_0 = \gamma_1 = 100$. We also observe the same convergence, supercloseness, and superconvergence phenomena for three meshes as predicted in our theoretical analysis.

Table 3. Rates of errors for Example 3 based on square and rectangular meshes with penalty parameters $\gamma_0 = \gamma_1 = 100$.

h_y	De	Rate	$D^{\Pi}e$	Rate	$D^{\mathcal{J}}e$	Rate	
1/8	1/8	3.4465×10^{-1}		3.1674×10^{-1}		3.1945×10^{-1}	
1/16	1/16	1.3095×10^{-1}	1.3961	1.1489×10^{-1}	1.4629	1.1297×10^{-1}	1.4996
1/32	1/32	5.3084×10^{-2}	1.3026	4.0167×10^{-2}	1.5162	3.8787×10^{-2}	1.5423
1/64	1/64	2.3179×10^{-2}	1.1954	1.4131×10^{-2}	1.5070	1.4416×10^{-2}	1.4279
1/8	1/16	2.1853×10^{-1}		1.9994×10^{-1}		1.9957×10^{-1}	
1/16	1/32	9.1487×10^{-2}	1.2561	7.4441×10^{-2}	1.4254	7.2634×10^{-2}	1.4582
1/32	1/64	3.9748×10^{-2}	1.2026	2.8217×10^{-2}	1.3995	2.9227×10^{-2}	1.3133
1/64	1/128	1.7577×10^{-2}	1.1771	9.6124×10^{-3}	1.5536	1.0655×10^{-2}	1.4557
1/12	1/8	2.5133×10^{-1}		2.2064×10^{-1}		2.7792×10^{-1}	
1/24	1/16	9.8588×10^{-2}	1.3500	8.0975×10^{-2}	1.4461	8.5858×10^{-2}	1.6946
1/48	1/32	4.2002×10^{-2}	1.2309	2.9083×10^{-2}	1.4772	3.2786×10^{-2}	1.3888
1/96	1/64	1.9020×10^{-2}	1.1429	1.0599×10^{-2}	1.4561	1.1400×10^{-2}	1.5239

In the three examples, the performance of errors De , $D^{\Pi}e$ and $D^{\mathcal{J}}e$ on both the square meshes and rectangular meshes is tested. The numerical results show that the nonconforming cut finite element method converge with optimal rate $O(h)$ for De and with $O(h^{3/2})$ order of convergence for $D^{\Pi}e$ and $D^{\mathcal{J}}e$, which is accordant with our theoretical results.

6. Conclusions

In this work, we have studied the superconvergence of the modified nonconforming cut finite element method to solve elliptic problems on rectangular meshes. We have proven that the supercloseness rate between the gradient of the numerical solution and the gradient of exact solution’s interpolation is $O(h^{3/2})$. Through a constructed postprocessing operator, we have proven that the error between the exact gradient and the postprocessed gradient with rate $O(h^{3/2})$. Numerical examples with squares and rectangular meshes have been provided to illustrate the theoretical results.

Author Contributions: Methodology, X.H. and F.S.; Writing—original draft, X.H.; Writing—review & editing, F.S. All authors have read and agreed to the published version of the manuscript.

Funding: The work of the first author is supported by the National Natural Science Foundation of China grant 12201312. The work of the second author is supported by the National Natural Science Foundation of China grant 12201303.

Data Availability Statement: The original contributions presented in the study are included in the article, further inquiries can be directed to the corresponding author.

Acknowledgments: We would like to thank the anonymous referees for their insightful suggestions and comments, which lead to a great improvement of the paper.

Conflicts of Interest: The authors declare no conflicts of interest.

References

1. Hansbo, A.; Hansbo, P. An unfitted finite element method, based on Nitsche's method, for elliptic interface problems. *Comput. Methods Appl. Mech. Eng.* **2002**, *191*, 5537–5552. [[CrossRef](#)]
2. Burman, E.; Hansbo, P. Fictitious domain finite element methods using cut elements: I. A stabilized Lagrange multiplier method. *Comput. Methods Appl. Mech. Eng.* **2010**, *199*, 2680–2686. [[CrossRef](#)]
3. Hansbo, P.; Larson, M.G.; Zahedi, S. A cut finite element method for a Stokes interface problem. *Appl. Numer. Math.* **2014**, *85*, 90–114. [[CrossRef](#)]
4. Huang, P.; Wu, H.; Xiao, Y. An unfitted interface penalty finite element method for elliptic interface problems. *Comput. Methods Appl. Mech. Eng.* **2017**, *323*, 439–460. [[CrossRef](#)]
5. Wang, N.; Chen, J. A nonconforming Nitsche's extended finite element method for Stokes interface problems. *J. Sci. Comput.* **2019**, *81*, 342–374. [[CrossRef](#)]
6. Massing, A.; Schott, B.; Wall, W.A. A stabilized Nitsche cut finite element method for the Oseen problem. *Comput. Methods Appl. Mech. Eng.* **2018**, *328*, 262–300. [[CrossRef](#)]
7. Burman, E.; Claus, S.; Hansbo, P.; Larson, M.G.; Massing, A. CutFEM: Discretizing geometry and partial differential equations. *Int. J. Numer. Methods Eng.* **2015**, *104*, 472–501. [[CrossRef](#)]
8. Lin, Q.; Yan, N. *The Construction and Analysis of High Efficiency Finite Element Methods*; Hebei University Publishers: Baoding, China, 1996. (In Chinese)
9. Zienkiewicz, O.C.; Zhu, J.Z. The superconvergent patch recovery and a posteriori error estimates. I. the recovery technique. *Int. J. Numer. Methods Eng.* **1992**, *33*, 1331–1364. [[CrossRef](#)]
10. Naga, A.; Zhang, Z. A posteriori error estimates based on the polynomial preserving recovery. *SIAM J. Numer. Anal.* **2004**, *42*, 1780–1800. [[CrossRef](#)]
11. Bank, R.E.; Xu, J.; Zheng, B. Superconvergent derivative recovery for lagrange triangular elements of degree p on unstructured grids. *SIAM J. Numer. Anal.* **2007**, *45*, 2032–2046. [[CrossRef](#)]
12. Lin, Q.; Tobiska, L.; Zhou, A. Superconvergence and extrapolation of non-conforming low order finite elements applied to the poisson equation. *IMA J. Numer. Anal.* **2005**, *25*, 160–181. [[CrossRef](#)]
13. Mao, S.; Chen, S.; Shi, D. Convergence and superconvergence of a nonconforming finite element on anisotropic meshes. *Int. J. Numer. Anal. Model.* **2007**, *4*, 16–38.
14. Hu, J.; Ma, R. Superconvergence of both the Crouzeix-Raviart and morley elements. *Numer. Math.* **2016**, *132*, 491–509. [[CrossRef](#)]
15. Li, Y. Superconvergent flux recovery of the Rannacher-Turek nonconforming element. *J. Sci. Comput.* **2021**, *87*, 32. [[CrossRef](#)]
16. Ming, P.; Shi, Z. Superconvergence studies of quadrilateral nonconforming rotated Q1 elements. *Int. J. Numer. Anal. Model.* **2006**, *3*, 322–332.
17. Stein, E. *Singular Integrals and Differentiability Properties of Functions*; Princeton University Press: Princeton, NJ, USA, 1970; Volume 30.
18. Gilbarg, D.; Trudinger, N.S. *Elliptic Partial Differential Equations of Second Order*, 2nd ed.; Springer: Berlin, Germany, 1983; Volume 224.
19. He, X.; Song, F.; Deng, W. A well-conditioned, nonconforming Nitsche's extended finite element method for elliptic interface problems. *Numer. Math. Theory Methods Appl.* **2020**, *13*, 99–130.
20. Arnold, D.; Boffi, D.; Falk, R. Approximation by quadrilateral elements. *Math. Comput.* **2002**, *71*, 909–922. [[CrossRef](#)]
21. He, X.; Chen, Y.; Ji, H.; Wang, H. Superconvergence of unfitted rannacher-turek nonconforming element for elliptic interface problems. *Appl. Numer. Math.* **2024**, *203*, 32–51. [[CrossRef](#)]

Disclaimer/Publisher's Note: The statements, opinions and data contained in all publications are solely those of the individual author(s) and contributor(s) and not of MDPI and/or the editor(s). MDPI and/or the editor(s) disclaim responsibility for any injury to people or property resulting from any ideas, methods, instructions or products referred to in the content.